

Supporting Information

Zeolite Encapsulated Ni(II) Schiff-Base Complexes: Improved Catalysis and Site Isolation

Susheela Kumari^a and Saumi Ray^{*a}

^aBirla Institute of Technology and Science, Pilani, Rajasthan 333031.

Physical Measurements

The XRD patterns were recorded by a RIGAKU MINIFLEX II X-ray diffractometer using a Cu K α X-ray source ($\lambda = 1.542 \text{ \AA}$) ranging 2θ from 8° to 50° at a scanning rate of 2° min^{-1} . The FESEM-EDX analysis was carried out by using a Zeiss EVO 40 instrument with an accelerated voltage of 5–20 kV and samples were gold-coated before analysis. The N₂ sorption isotherms and Brunauer–Emmett–Teller (BET) surface area and pore volume were recorded on a Quantachrome instruments along with a volumetric adsorption setup at -196°C . Thermogravimetric (TGA) analysis was performed in inert atmosphere within the temperature range of (25–800) $^\circ\text{C}$ by using a TGA-60, SHIMADZU equipment at a heating rate of $10^\circ\text{C min}^{-1}$. The FT-IR measurements were carried out on an ABB FTIR spectrometer with a DRIFT accessory in the range of (450–4000) cm^{-1} by using KBr as a reference. X-ray photoelectron spectroscopic measurement (XPS) was performed on a commercial Omicron EA 125 spectrometer with an Mg K α X-ray source (1253.6 eV). Samples were used in form of pellets after neutralization and kept in a vacuum oven overnight before XPS. High-resolution XPS traces were deconvoluted by using the Gaussian and Lorentzian statistical analysis in Origin-9 software. The solution UV-vis absorption spectra were recorded by using Shimadzu UV-2100 spectrophotometer. The solid-state UV-vis spectra were performed on a Shimadzu UV-2450 spectrophotometer in reflectance mode by using barium sulfate as a reference. UV-vis spectrophotometer is equipped with an integrating sphere of 60 mm inner diameter and Kubelka–Munk analysis is performed on the reflectance data. The KM factor, $F(R)$, is given by $F(R) = (1 - R)^2 / 2R = k/s$ where R is the diffuse reflectance of the sample as compared to BaSO₄, k is the molar absorption coefficient, and s is the scattering coefficient of the sample. GC chromatographic experiments were performed on a Shimadzu GC-2014 by using a FID detector for the catalysis study of neat and encapsulated nickel (II) Schiff-base complexes.

Figure S1:

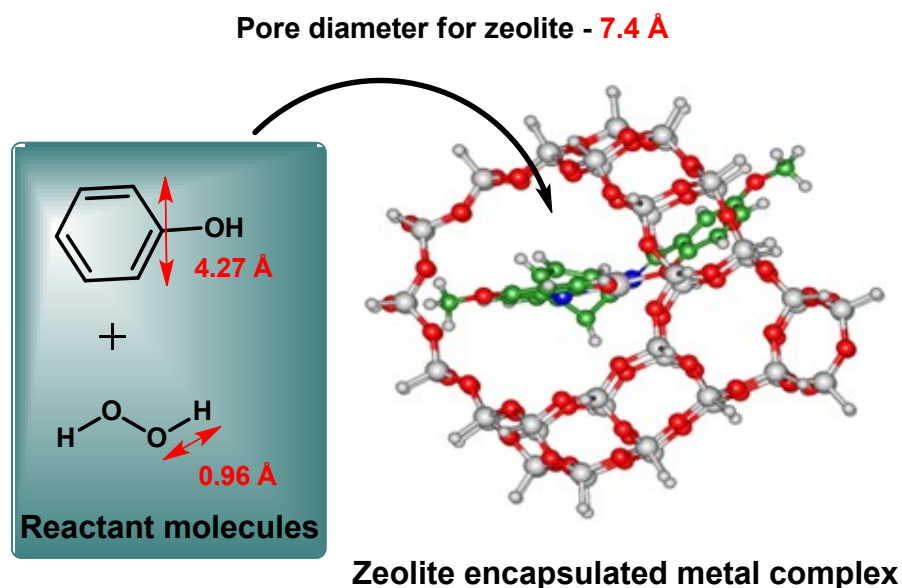


Figure S1: Schematic representation of zeolite encapsulated nickel (II) Schiff-base complex and reactant molecules (phenol and H₂O₂).

Experimental section

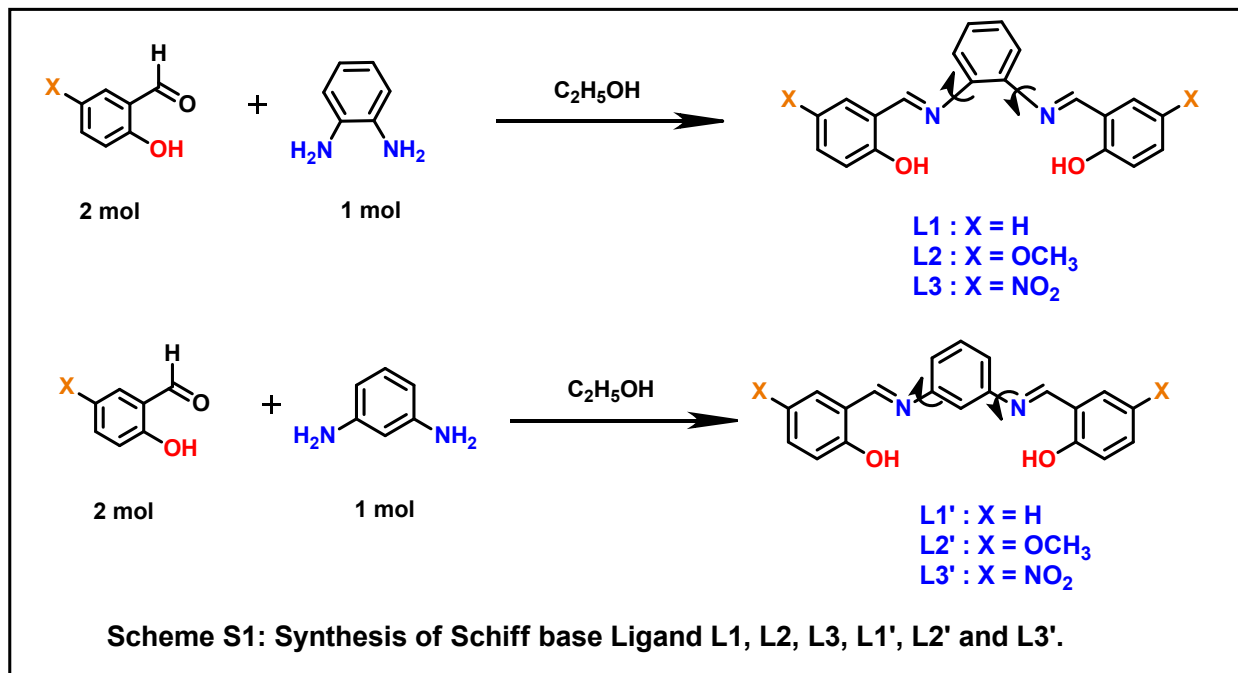
Materials and preparation

The Na-zeolite-Y, 5-hydroxy salicylaldehyde, 2-hydroxy-5-methoxy benzaldehyde, 2-hydroxy-5-nitro benzaldehyde, 1,2- Phenylenediamine and 1,3- Phenylenediamine are purchased from Sigma-Aldrich, India. Nickel acetate and all solvents like ethanol, acetone, methanol, ether and acetonitrile are procured from S.D. fine, India.

Preparation of the ligands and Ni (II)–Schiff base complexes^{1,2}

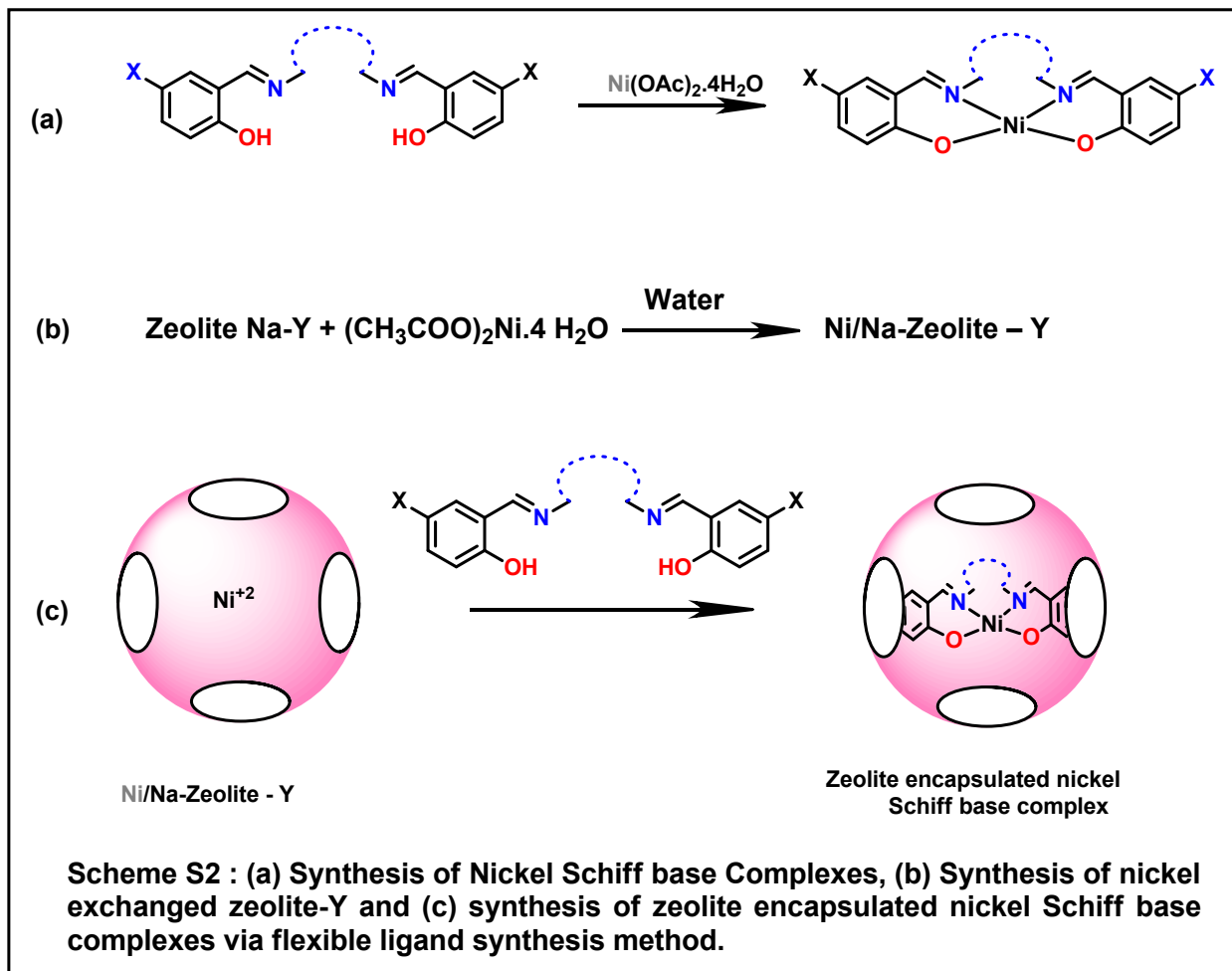
10 mmol of 1,2-phenylenediamine or 1,3-phenylenediamine and 20 mmol of salicylaldehyde / its derivatives are stirred at 70 °C under refluxing condition for 4 h with ethanol as solvent. At the end of the reaction, the product is filtered out, washed with ethanol and finally air-dried (Scheme S1).

Scheme S1:



An equimolar ratio of the Schiff-base ligand and nickel acetate in ethanol are refluxed at 80 °C for 3 h. The reaction mixture then is cooled and filtered out. Finally, product is washed with ethanol and dried under vacuum (Scheme S2).

Scheme S2:



Preparation of the Ni(II) exchanged zeolite -Y³

To synthesize a Ni (II) exchanged zeolite -Y, 10 g of zeolite -NaY is suspended in a 0.01 M of nickel(II) acetate solution and reaction mixture is stirred at room temperature for 24 h. The slurry is filtered and washed with distilled water, and finally dried for 12 h in muffle furnace at 150°C to obtain Ni (II) - exchanged zeolite-NaY.

Preparation of the encapsulated Ni(II)-Schiff base complexes in zeolite Y^{4,5}

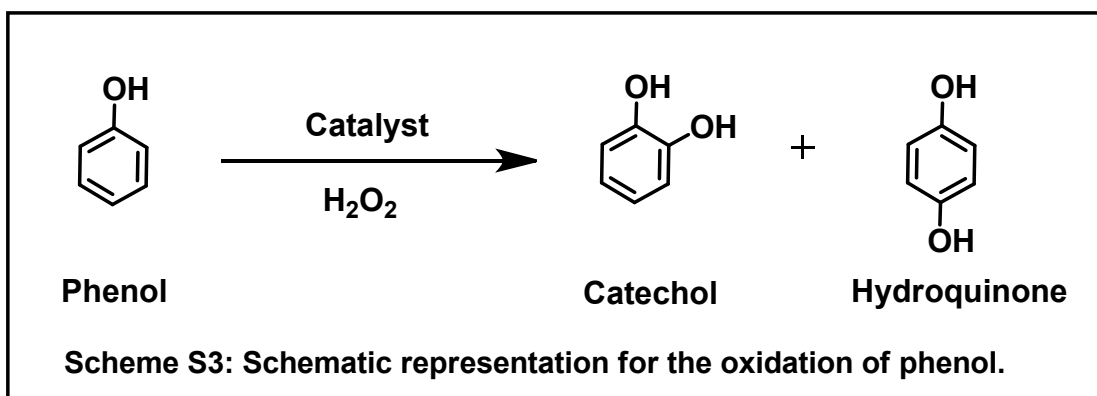
Encapsulated Ni(II) Schiff-base complexes are synthesized by using 'flexible ligand method' following the previously reported literature report. A stoichiometric excess of the Schiff-base ligand is allowed to diffuse through the pores of the Ni(II) -exchanged zeolite Y by melting it at high temperature. The reaction mixture is refluxed for 24 h. Schiff-base ligand reacts with nickel ion already present inside zeolite-Y, complex formation takes place inside the cavities. To remove the impurities present in form of unreacted and adsorbed surface species, product is repeatedly washed with acetone, methanol and diethyl ether by using Soxhlet extraction apparatus. The synthesized product finally is treated with 0.01 M NaCl solution for 12 h at room temperature to remove the unreacted nickel

ions. The resultant product is filtered and finally repeatedly washed with distilled water till the filtrate is negative for the chloride ion test. Finally, the product is dried in muffle furnace for 10–12 h at 150 °C.

Catalytic reaction

To carry out the catalytic hydroxylation of phenol 0.05 g of catalyst, 2 ml of acetonitrile as a solvent, 6.16 mmol of phenol, and 2.54 ml of 30% H₂O₂ as an oxidant are added and the reaction mixture is refluxed with constant stirring for 6 h at 80°C (Scheme S3). The progress of reaction is monitored by Gas chromatography (GC). At the end of the reaction, the solid catalyst is extracted by filtration and washed with solvents and the supernatant solution of the reaction mixture is analyzed by Gas chromatography after centrifugation.

Scheme S3:



X-ray Diffraction (XRD) studies

Figure S2:

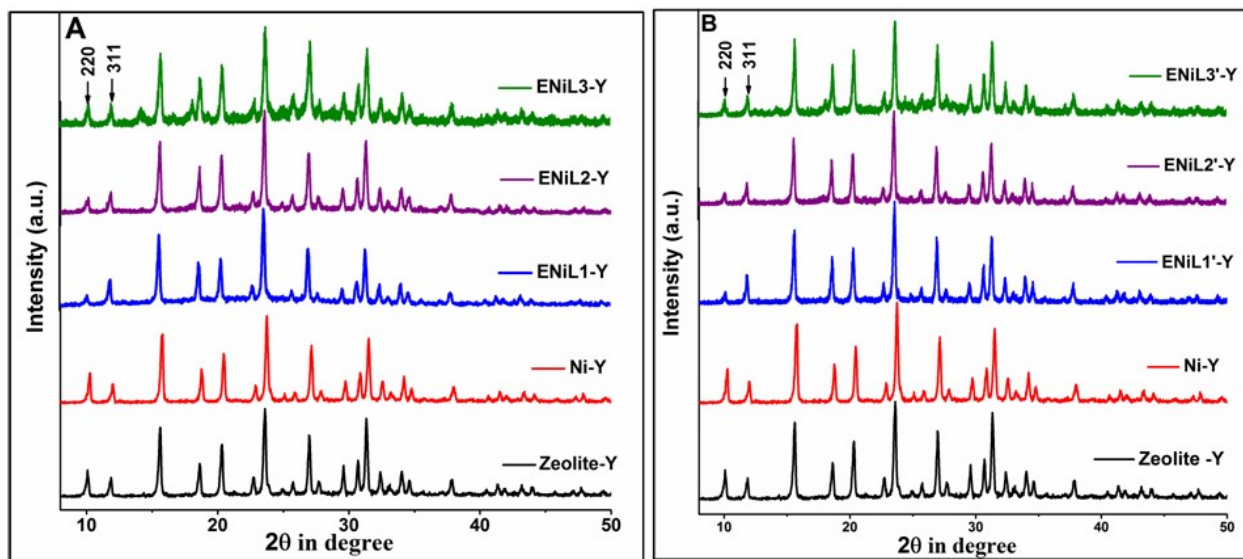


Figure S2: (A) XRD patterns of pure zeolite-Y, Ni-exchanged zeolite -Y, ENiL1-Y, ENiL2-Y and ENiL3-Y and (B) XRD patterns of pure zeolite-Y, Ni-exchanged zeolite -Y, ENiL1'-Y, ENiL2'-Y and ENiL3'-Y.

FTIR Spectroscopic Study

Figure S3:

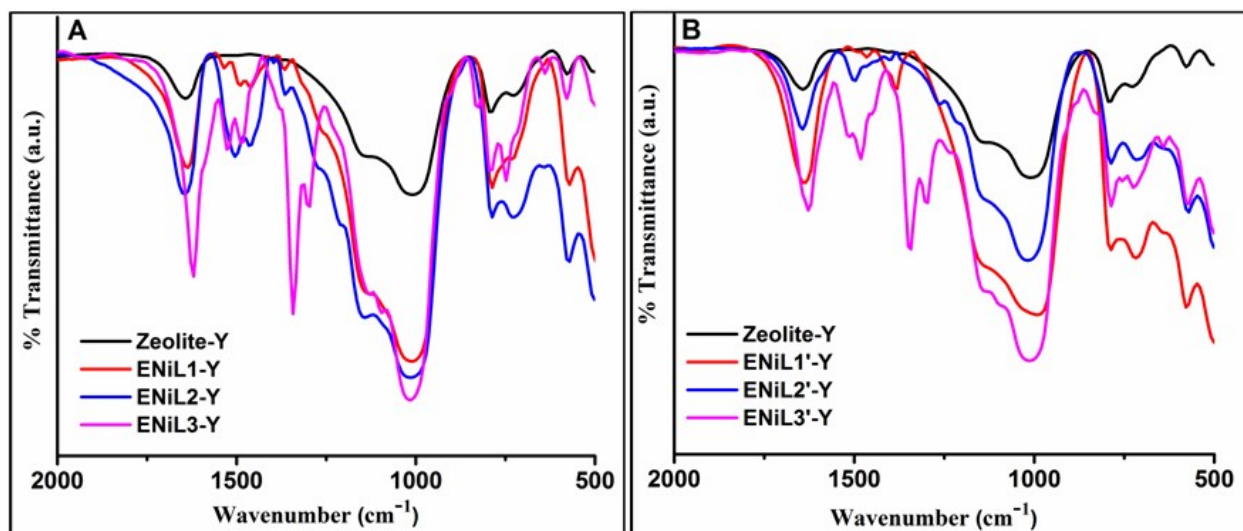


Figure S3: FTIR spectra of (A) pure zeolite-Y, ENiL1-Y, ENiL2-Y and ENiL3-Y and (B) pure zeolite-Y, ENiL1'-Y, ENiL2'-Y and ENiL3'-Y.

Table S1. FTIR data of neat and encapsulated complexes.

S. No	Samples	C=N	C=C stretching	ν_{C-H}	C-O stretching
-------	---------	-----	----------------	-------------	----------------

		stretching		deformation	
1	NiL1	1605	1520, 1443	1381	1296
2	ENiL1-Y	1636	1489, 1458	1396	1292
3	NiL2	1605	1528, 1466	1381	1277
4	ENiL2-Y	1643	1504, 1458	1396	1265
5	NiL3	1612	1543, 1481	1381	1257
6	ENiL3-Y	1620	1528, 1489	1389	1254
7	NiL1'	1589	1543, 1466	1389	1250
8	ENiL1'-Y	1643	1489, 1458	1358	1292
9	NiL2'	1589	1516, 1474	1381	1273
10	ENiL2'-Y	1643	1497, 1442	1396	1265
11	NiL3'	1612	1528, 1482	1372	1256
12	ENiL3'-Y	1628	1520, 1481	1342	1296

Thermal analysis

To determine the thermal stability of neat and encapsulated Ni(II) Schiff-base complexes thermo-gravimetric (TGA) analysis has been done in the temperature range of (25 – 800)°C under inert atmosphere with a heating rate of 10 °C/minute (The TGA plots of zeolite -Y, free state and encapsulated nickel complexes presented in Figure S4. The neat complexes show weight loss only due to decomposition of ligand moiety whereas all encapsulated nickel complexes show an additional weight loss in the temperature range of (30 – 185) °C due to loss of intrazeolite water molecules. The second step of weight loss widens in the temperature range of (300 – 780) °C suggesting slow decomposition of coordinated ligand and is of relatively lesser extent in comparison to the corresponding free state nickel complexes. These results indicate the presence of low loading level of nickel complex inside the supercage of zeolite Y and well in agreement with the results obtained by the EDX analysis. Encapsulated systems show the decomposition temperature extends towards higher temperature, which is the indication of thermal stability of the encapsulated nickel complexes.

Figure S4:

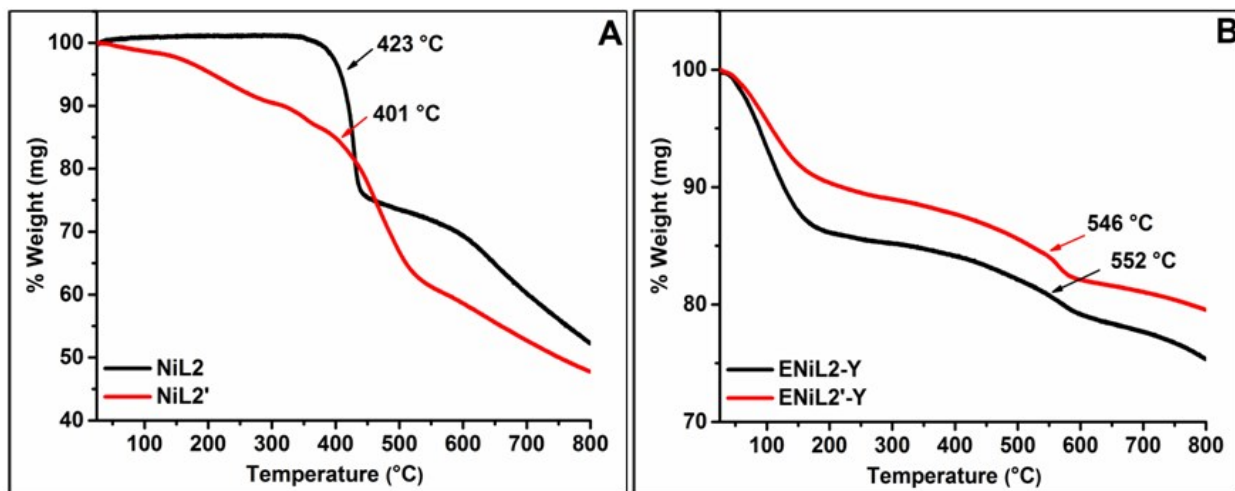


Figure S4: Thermogravimetric analysis (TGA) results for (A) NiL2 and NiL2' free state complex and (B) ENiL2-Y and ENiL2'-Y encapsulated complex.

Figure S5:

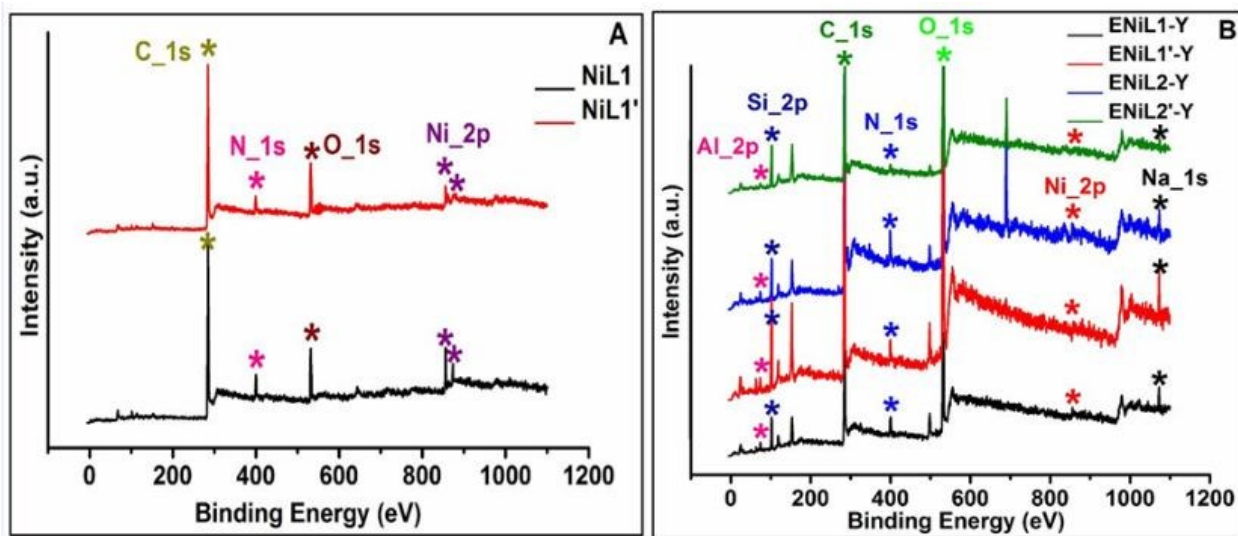


Figure S5: XPS survey spectra of (A) neat complexes NiL1 and NiL1' (B) encapsulated complexes ENiL1-Y, ENiL1'-Y, ENiL2-Y and ENiL2'-Y.

Figure S6:

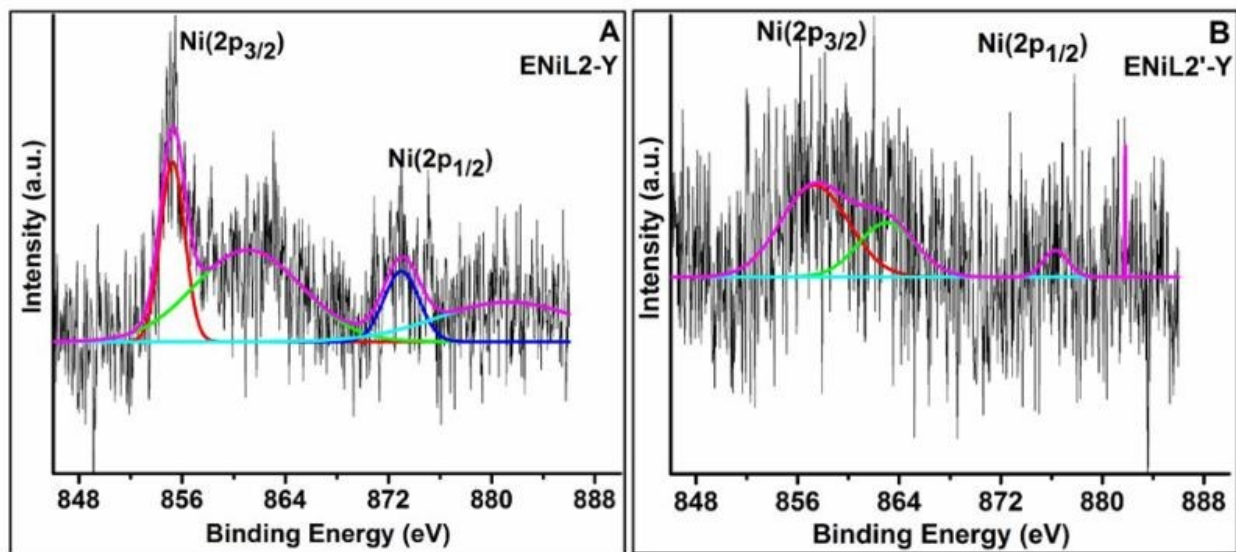


Figure S6: High-resolution XPS signals of Ni (2p) of (A) ENiL2-Y and (B) ENiL2'-Y.

Figure S7:

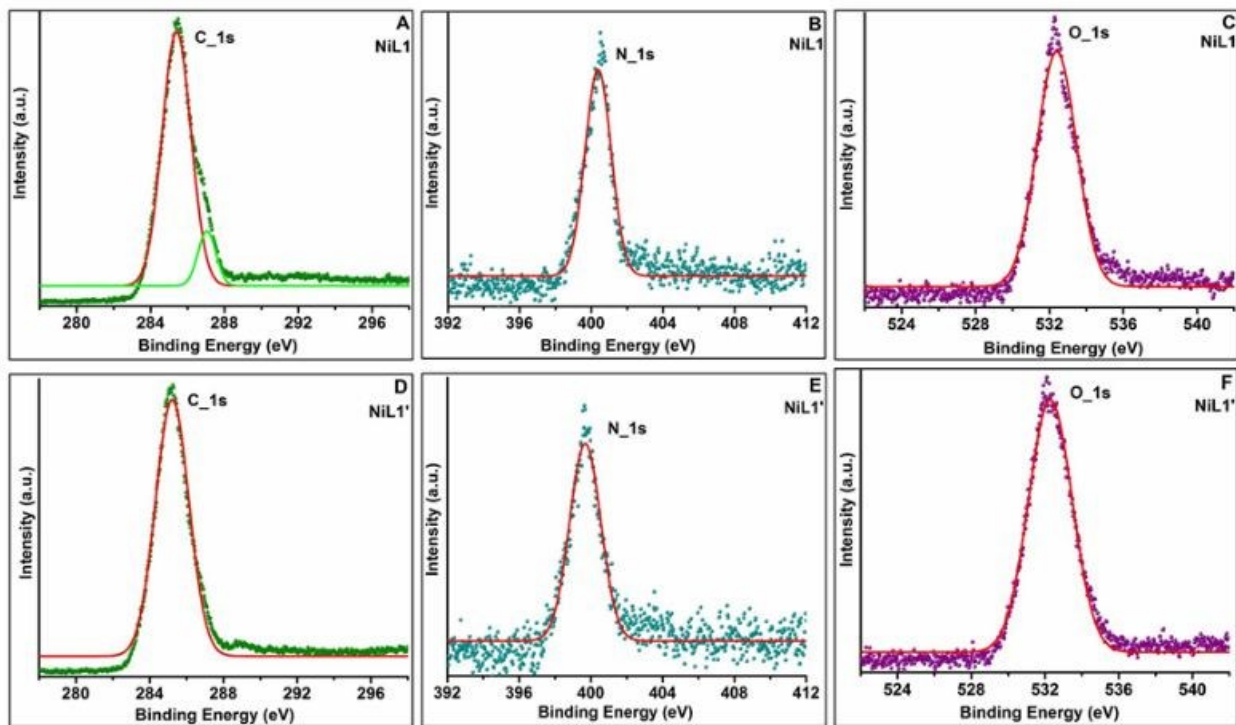


Figure S7: High-resolution XPS spectra of C (1s), N (1s), and O (1s) for NiL1 and NiL1' complex.

Figure S8:

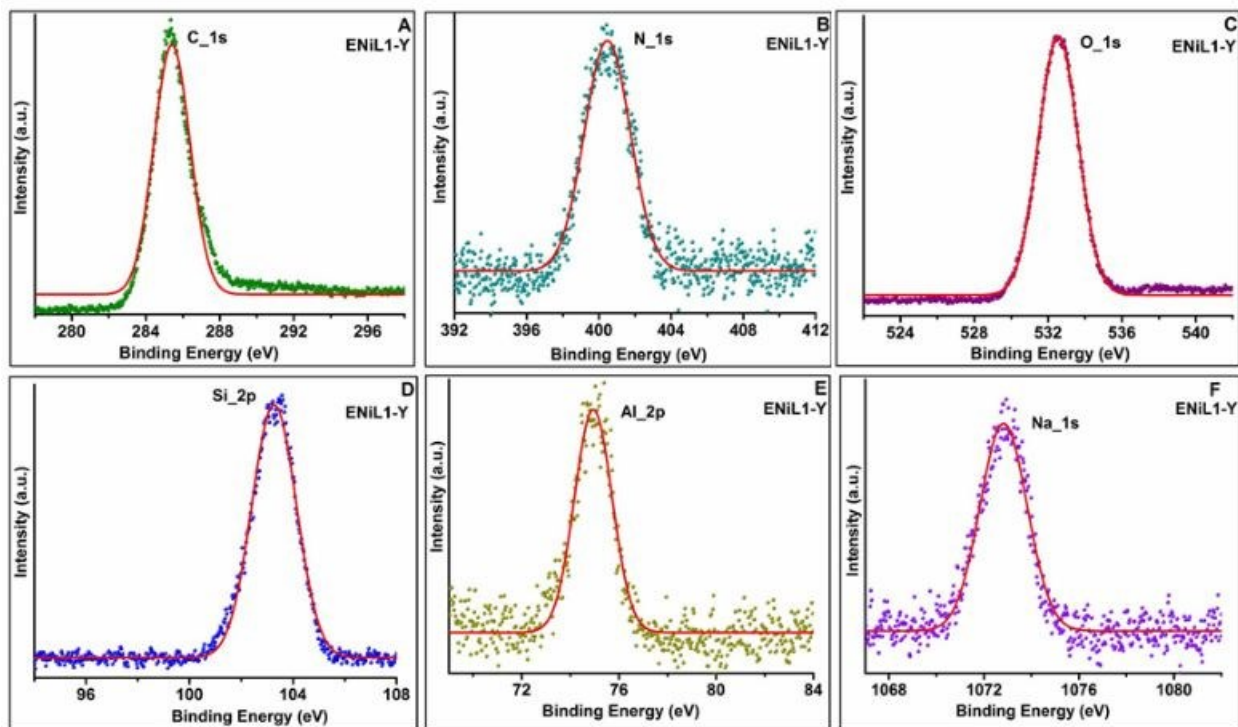


Figure S8: High-resolution XPS spectra of C (1s), N (1s), O (1s), Si (2p), Al (2p) and Na (1s) for ENiL1-Y complex.

Figure S9:

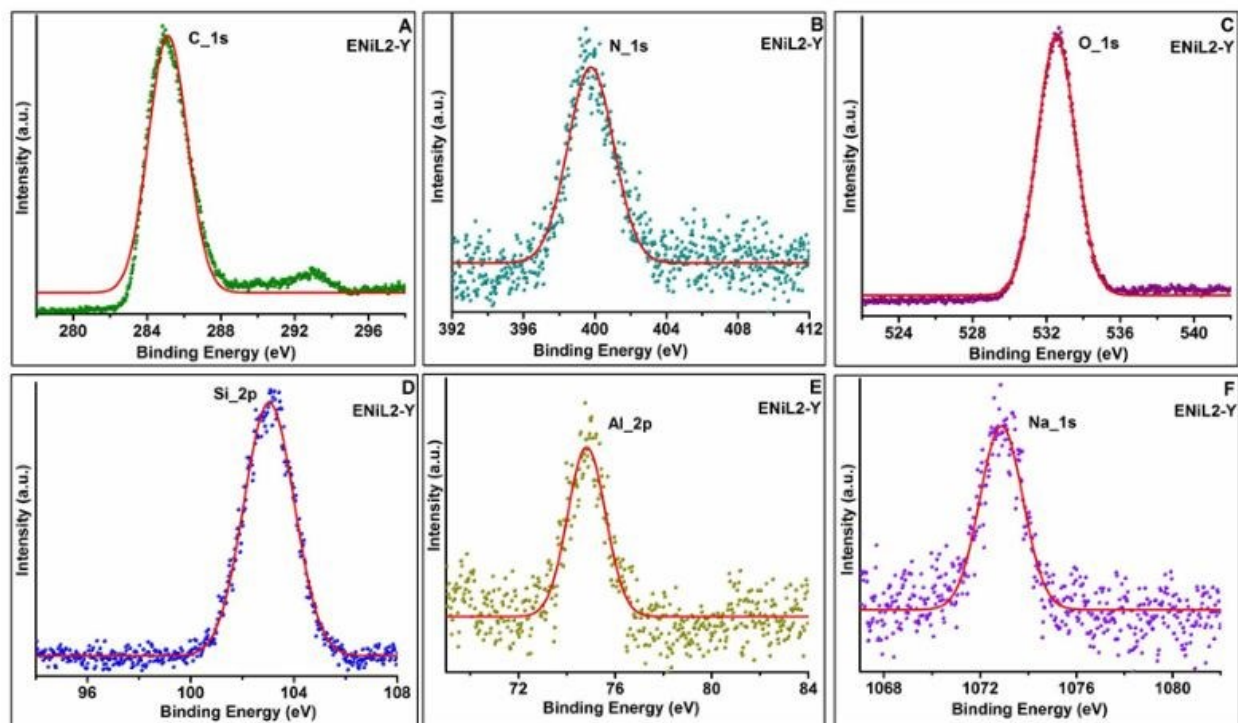


Figure S9: High-resolution XPS spectra of C (1s), N (1s), O (1s), Si (2p), Al (2p) and Na (1s) for ENiL2-Y complex.

Figure S10:

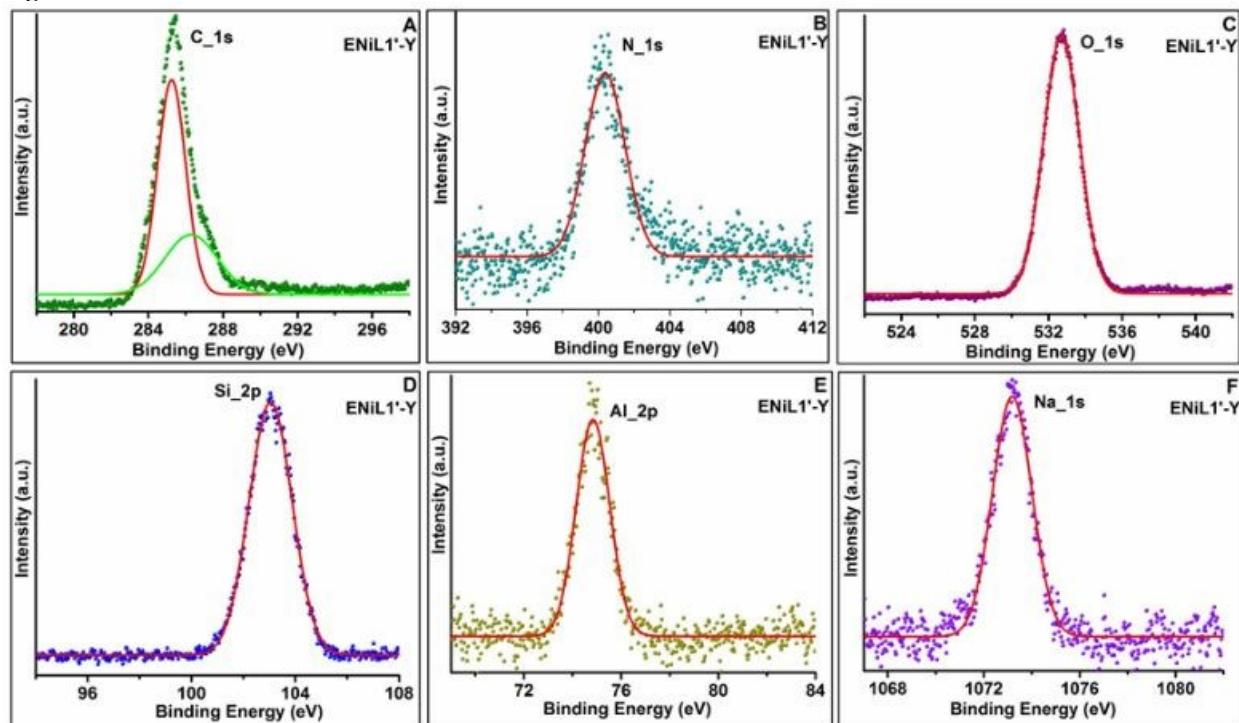


Figure S10: High-resolution XPS spectra of C (1s), N (1s), O (1s), Si (2p), Al (2p) and Na (1s) for ENiL1'-Y complex.

Figure S11:

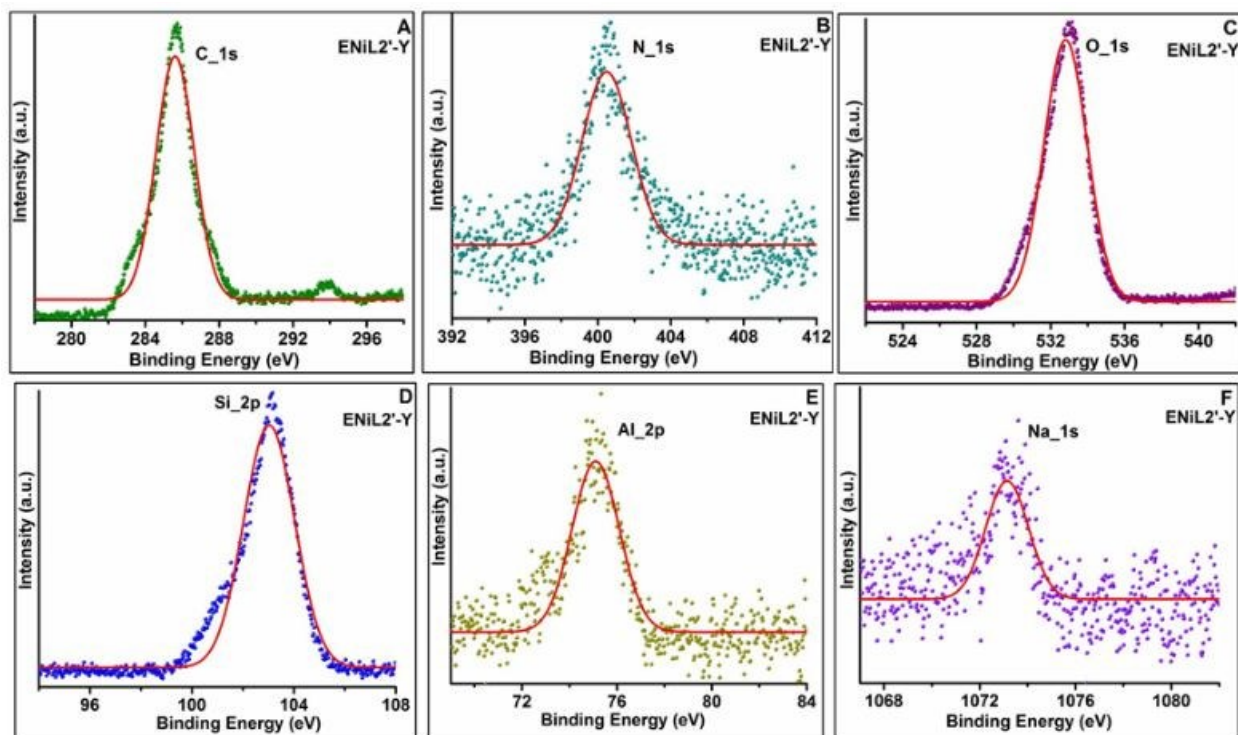


Figure S11: High-resolution XPS spectra of C (1s), N (1s), O (1s), Si (2p), Al (2p) and Na (1s) for ENiL2'-Y complex.

Figure S12:

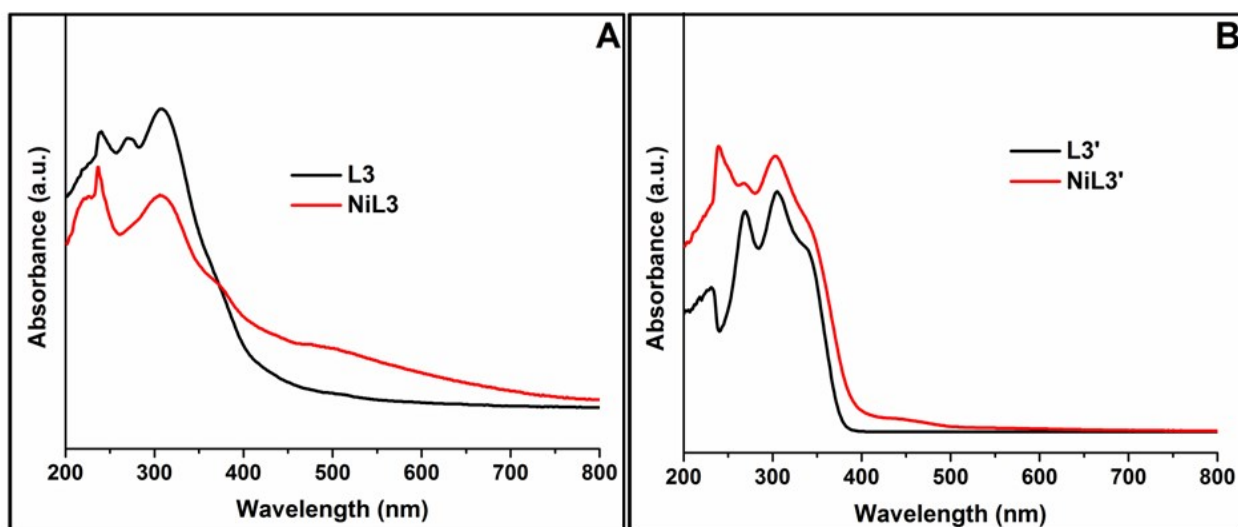


Figure S12: Solution UV-vis spectra of (A) L3 and NiL3 and (B) L3' and NiL3'.

Figure S13:

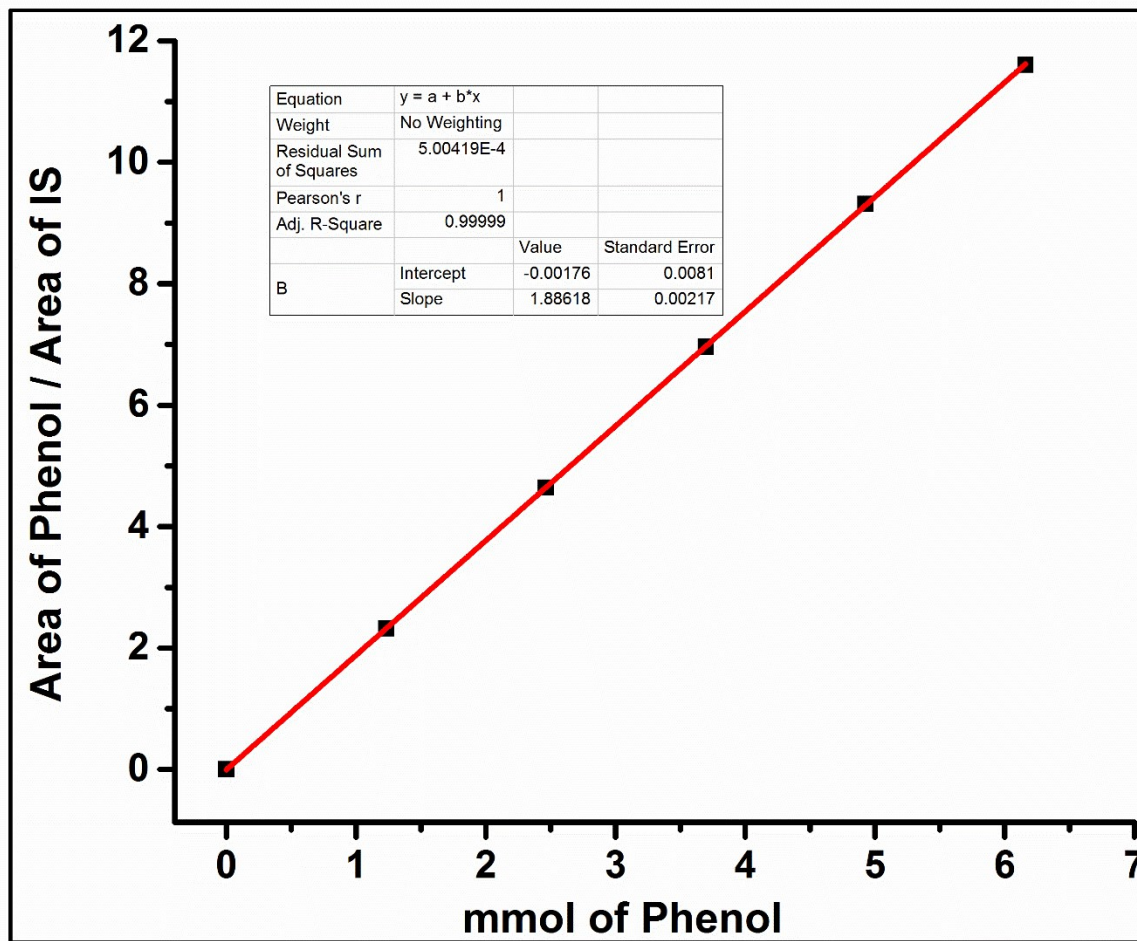


Figure S13: Calibration curve of phenol.

Figure S14:

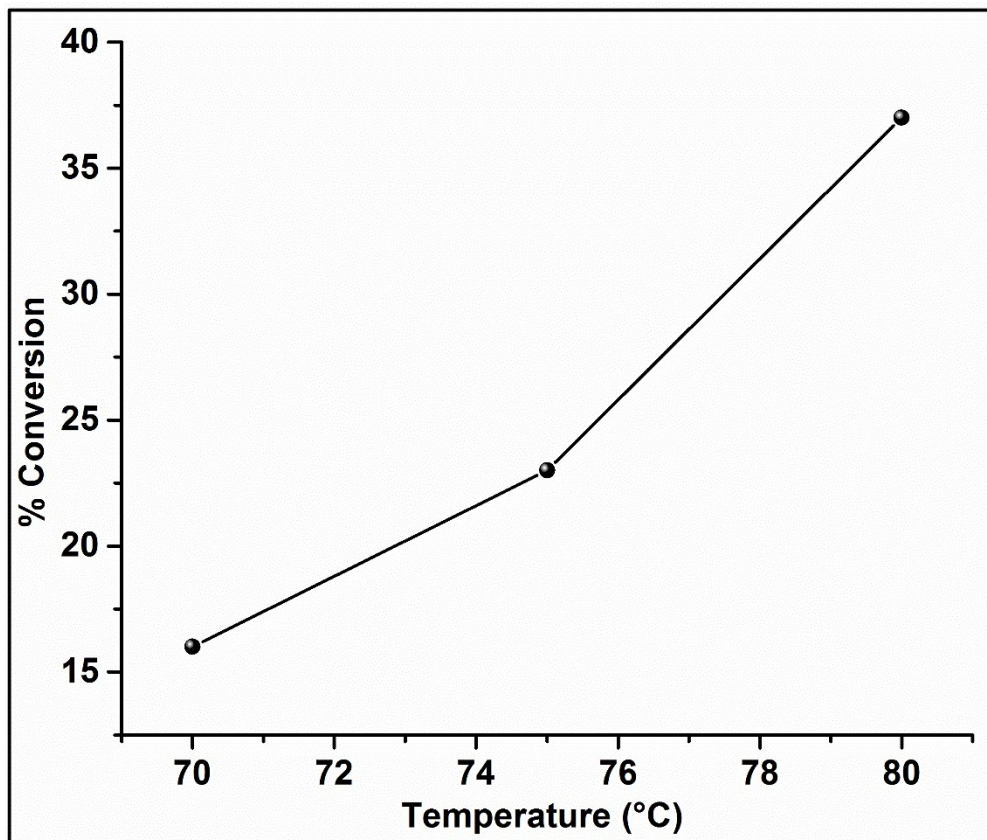


Figure S14: % Conversion of phenol oxidation with respect to temperature.

Figure S15:

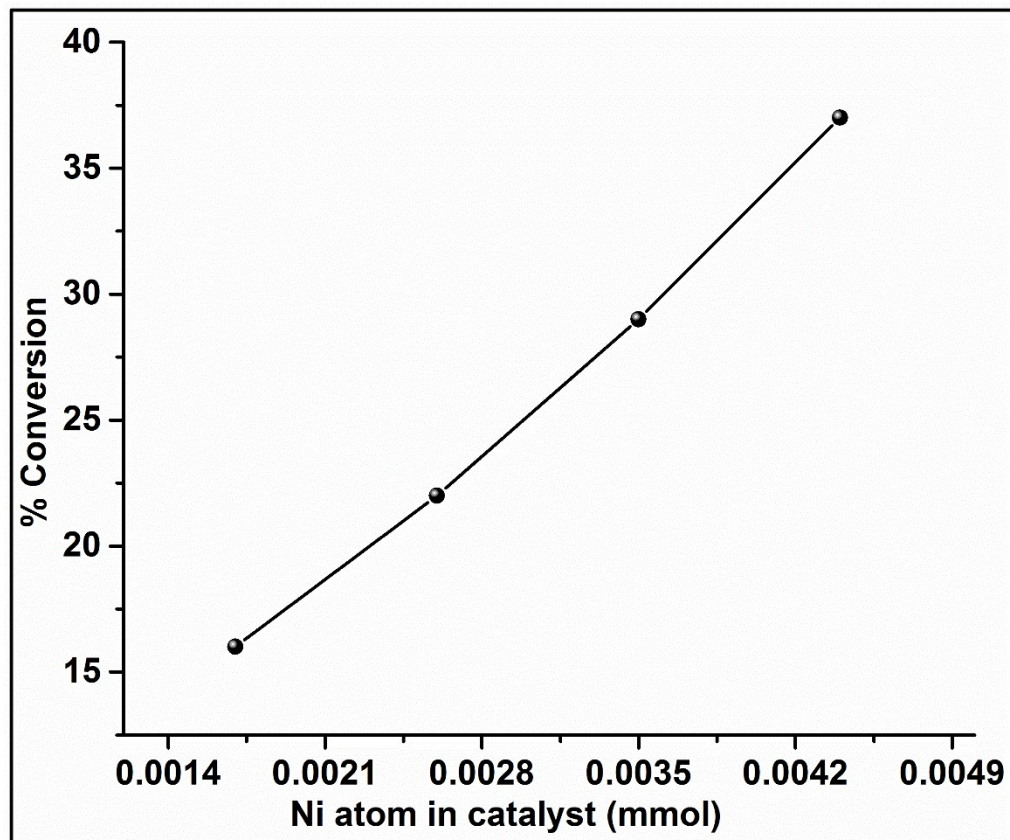


Figure S15: % Conversion of phenol oxidation with respect to amount of catalyst.

Table S2. Oxidation of phenol catalyzed by encapsulated nickel salophen complexes along with efficiency of hydrogen peroxide.

S. No	Samples	Ni ²⁺ in catalyst (mmol) ^[a]	% Conversion	TON ^[b]	Selectivity		H ₂ O ₂ efficiency ^[c]
					Catechol	Hydroquinone	
1	ENiL1-Y	0.00443	37	514.6	75	25	64.8
2	ENiL1'-Y	0.00468	32	421.4	74	26	65.7
3	ENiL2-Y	0.00460	43	576.1	72	28	64.4
4	ENiL2'-Y	0.00477	39	503.8	76	24	66.7

Reaction conditions: Phenol (0.58 g, 6.16 mmol), H₂O₂ (2.54 ml (30%)), acetonitrile 2 ml, temperature 80 °C, catalyst (0.05 g for encapsulated complexes and 0.025 g for neat complexes), Reaction time-6 h. [a] mmol of Ni atom calculated in 0.025 g for neat complexes and 0.05 g for encapsulated complexes). [b] TON (turn over number): Turnover number calculated at the completion of reaction (mmol of phenol transformed / mmol of nickel metal in catalyst). [c] H₂O₂ efficiency = (moles of hydroxylation products of phenol formed / moles of H₂O₂ consumed) × 100.

Table S3. Comparison of zeolite based catalysts performances for the phenol hydroxylation reaction.^[a]

S.No.	Catalyst	Catalyst amount ^[b]	PhOH ^[c]	Time (h)	Conversion (%) ^[d]	Ref.
1	Ti-SBA-12	100	3:1	12	15.0	6
2	Fe(Hybe.2H ₂ O)Cl-Y	25	1:1	6	43.4	7
3	[Cr(Hybe)·2H ₂ O]Cl-Y	25	1:1	6	32.8	7
4	[Cu(sal-ambmz)Cl]-Y	25	1:3	6	42.0	8
5	CuCl ₁₄ Pc-NaY	750	2:1	8	21.4	9
6	Cu(NO ₂) ₄ Pc-NaY	750	1:1	8	10.8	9
7	[Ni(Pic) ₂]-Y ^[e]	15	1:1	1.16	-	10
8	ENiL2-Y	50	1:3.6	6	43.0	This work

[a]Oxygen source H₂O₂, solvent ACN, temperature 80°C, Hybe stands for 1,2-bis(2-hydroxybenzamido)ethane, sal-ambmz stands for (salicylaldehyde and 2-aminomethylbenzimidazole-based ligand), Pc stands for phthalocyanine and Pic stands for picolinato. [b] Catalyst amount in (mg). [c] PhOH/H₂O₂ molar ratio. [d] Conversion of PhOH (%). [e] Reaction mixture is subjected to microwave irradiation (280 W).

References

1. A. Choudhary, B. Das and S. Ray, *Dalton Trans.*, 2015, **44**, 3753-3763.
2. H.-C. Zhang, W.-S. Huang and L. Pu, *J. Org. Chem.*, 2001, **66**, 481-487.
3. A. Choudhary, B. Das and S. Ray, *Dalton Trans.*, 2016, **45**, 18967-18976.
4. A. Choudhary, B. Das and S. Ray, *Inorg. Chim. Acta*, 2017, **462**, 256-265.
5. K. K. Bania, D. Bharali, B. Viswanathan and R. C. Deka, *Inorg. Chem.*, 2012, **51**, 1657-1674.
6. A. Kumar and D. Srinivas, *J. Mol. Catal. A: Chem.*, 2013, **368**, 112-118.
7. M. R. Maurya, S. J. Titinchi and S. Chand, *J. Mol. Catal. A: Chem.*, 2004, **214**, 257-264.

8. M. R. Maurya, A. K. Chandrakar and S. Chand, *J. Mol. Catal. A: Chem.*, 2007, **263**, 227-237.
9. R. Raja and P. Ratnasamy, *Appl. Catal., A*, 1996, **143**, 145-158.
10. K. K. Bania and R. C. Deka, *J. Phys. Chem. C*, 2013, **117**, 11663-11678.